Published in Micro & Nano Letters
Received on 27th January 2010
Revised on 18th March 2010
doi: 10.1049/mnl.2010.0012

ISSN 1750-0443

Infrared-photovoltaic properties of graphene revealed by electro-osmotic spray direct patterning of electrodes

G. Hwang S. Haliyo S. Régnier

Institut des Systèmes Intelligents et de la Robotique, Université Pierre et Marie Curie, 4 Place Jussieu, 75005 Paris, France
E-mail: hwang@isir.upmc.fr

Abstract: Although two-dimensional thin-film nanostructures such as graphene are extremely promising for future optical or electronic devices, the required manufacturing technologies are still lacking. Herein the authors introduce a robotically controlled electro-osmotic spray deposition method of colloids with a high electric potential to create optoelectronic devices directly onto the surface of graphene. Since the process does not require a clean room or lithography method, pure graphene optoelectronic devices can be manufactured at a low cost. Moreover, preliminary experiments revealed that the manufactured graphene optoelectronic devices have excellent photoelectric properties in the infrared wavelengths.

1 Introduction

Graphene is a single atomic layer, two-dimensional nanostructure with carbon atoms in hexagonal honeycomb lattices [1]. Its specific properties, such as the charge carriers mimicking massless relativistic Dirac fermions, the anomalous quantum Hall effect and the ballistic transport even at room temperature [2–4], make graphene a promising building block for future electronics and nanoelectromechanical systems. Moreover, graphene also has remarkable photonic properties. It can absorb photons in wide wavelength range, from the visible to the infrared (IR) and also has one of the strongest interband transition among other materials [5, 6]. Therefore graphene is also very promising for optoelectronic or optomechatronic devices. However, the intrinsic optoelectronic properties of graphene, especially zero bandgap optoelectronic behaviour have not been studied thoroughly yet because of the difficulty to synthesise high-quality large-scale graphene optoelectronic devices and because of the challenges in device prototyping. The main difficulty in prototyping comes from the integration of electrodes in optoelectronic devices made from pure graphene. Photo/electro-beam lithography has been attempted as a first approach [5, 7, 8]. However, the applied photoresist can change the intrinsic physical properties of graphene. To avoid this problem, it is required to transfer graphene onto the electrodes, further complicating the process. Dielectrophoresis was often utilised as an alternative method to assemble graphene in aqueous solvents [9–14]. In this case, it is difficult to avoid the liquid residue trapped within the interfacial space between graphene and the target substrate. In both approaches, it is difficult to fabricate homogeneous graphene devices and the selective deposition of graphene with a given layer profile is limited. Robotic assembly could be attempted as an alternative way to transfer graphene as was demonstrated in other thin-film nanostructures [15]. Although it has high enough accuracy and repeatability, it is limited by low yield from serial assembly and errors caused by nonlinear physics during nanomanipulation. Another drawback of this method based on *in situ* scanning electron microscope nanomanipulation is its incompatibility with graphene synthesised over dielectric substrates. The mechanically delicate graphene can also be damaged during the transfer. Furthermore, the alignment between the graphene film and the target substrate presents additional technical challenges. In this Letter, a maskless writing technique of graphene optoelectronic devices based on gold nanoparticle ink spray is proposed. Gold nanoparticle ink solution-based microstructure patterning [16], device assembly [17], soldering [18] and nanowire growth [19] on other nanostructures have previously been

demonstrated. However, this contact-based deposition relies principally on capillary forces, and hence is inapplicable on graphene because of its extreme hydrophobicity. Electrospray methods can be considered to locally control the deposition [19] but it requires a very high potential (around 1 kV) between huge electrodes. Consequently, thermal evaporation of liquid solution caused by local joule heating from this high potential causes clogging at the capillary probe and prevents colloidal ejection. This limits the choice of liquid medium to high boiling point materials.

The present contribution describes a process for *in situ* non-contact, direct writing of graphene optoelectronic devices without the need of complicated clean room or vacuum conditions. The gold nanoink is sprayed onto graphene only by electrostatic force between the substrate and capillary probe and the electro-osmotic field inside the capillary. The setup is composed of an inverted Olympus IX71 microscope (Fig. 1), with a 25× OCTAX objective and a high-speed Dalsa Genie CMOS camera (1″, 1400 × 1024 pixels, 60 fps). An IR laser (CW 1480 nm, max power of 120 mW) from OCTAX Microscience GmbH is connected to the rear port of the microscope. The focused laser spot diameter is approximately a few microns. For gold nanoink spray deposition, a single Kleindiek (MM3A-EM) manipulator was used (Fig. 1). For probing and manipulating graphene, two of the same manipulators were used (Fig. 1). Each has three degrees of freedom and, respectively, 5, 3.5 and 0.25 nm resolution at the tip in the *X*, *Y* and *Z*-axis of inertial frame. Each axis is actuated and controlled with piezo stick-slip principle (Fig. 1). The current between two probes of manipulators could be measured with a high-resistance electrometer, Keithley 6517b. The graphene manufacturing setup shown in Fig. 1 has several functions including electrical probing, focused laser setup, gold nanoink deposition and mechanical manipulation. The nozzle head for spray is manufactured out of a borosilicate capillary tube using a micropipette puller (DMZ Universal Puller, Zeitz Instruments, Germany). Pipettes with 1 μm outer diameter and 500 nm inner diameter were fabricated. Conventionally, electrodes should be embedded on pipettes by metal deposition [19]. However, it is not necessary in this approach; thus, the liquid flow inside transparent pipette can be monitored. The pipettes were filled from the front end with two different types of gold nanoparticle suspension (ULVAC). The first one has a mean particle size of 3–7 nm, suspended in nonpolar *n*-tetradecane ($C_{14}H_{30}$). The other has a mean particle size of 2–4 nm, suspended in toluene (C_7H_8). The printing process is visualised by a charge-coupled device camera in the inverted optical microscope.

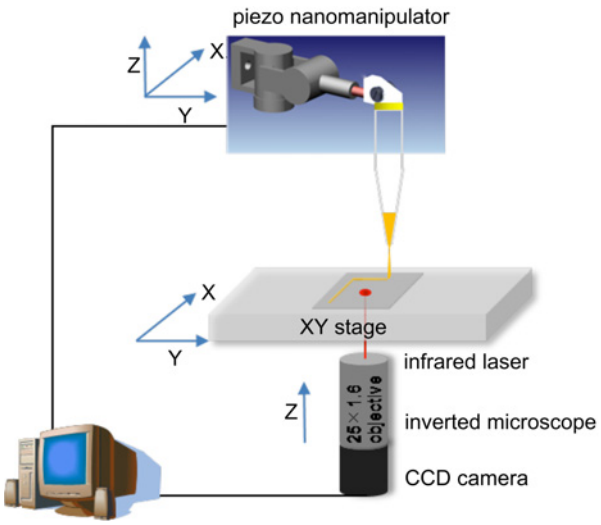

Figure 1 *Schematic of gold nanoparticle ink spray setup*

Fig. 2 shows schematically the processes of manufacture. A graphene sample was prepared on a glass Pyrex substrate. The sample preparation was inspired from the widely used anodic bonding process that is usually applied to bond single-crystal semiconductor wafer such as Si or GaAs to a Pyrex substrate (Fig. 2*a*). In this process, a very firm contact is obtained between the substrate and Si, owing to the formation of chemical bonds at the interface by an application of a potential difference in the order of a kV to the heated Pyrex/Si substrate. A similar mechanism was applied to the conducting materials that readily oxidise to bond to Pyrex substrates [20]. An anodic voltage (1.2–1.7 kV) was applied on the graphite sample with the cathode contacting the backside of the Pyrex substrate. The substrate was heated to around 200°C.

After the bonding is achieved, the bulk graphite sample can be cleaved off, leaving several bonded areas on the glass surface (Fig. 2*b*). These are then peeled off using an adhesive tape to leave many transparent areas with

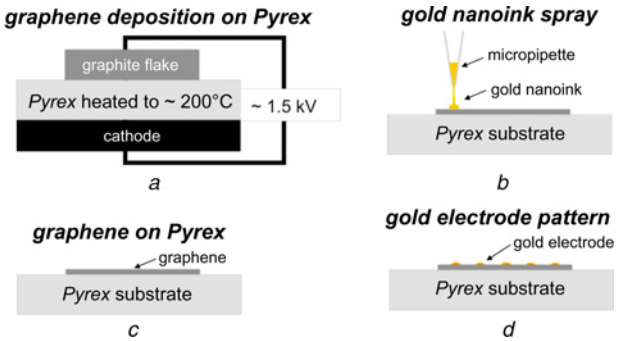

Figure 2 *Schematic process of creating graphene optoelectronic devices*

a Graphene synthesis onto Pyrex substrate using anodic bonding by applying 1.5 kV potential between graphite chuck and cathode placed around substrate
b Remaining graphene after mechanical exfoliation over Pyrex substrate
c Electrostatic force-assisted gold nanoink spray deposition onto graphene by micro-pipette and substrate
d Patterned gold electrodes onto graphene after annealing by laser

mono/multilayer graphene on Pyrex. Optical microscopy was used to pre-identify the graphene layer configurations from the reference contrast. Further Raman spectroscopy identification of different contrasts in different graphene layer configurations can be refereed elsewhere [20]. Large area, high-quality graphene sample was prepared for the conductometric property characterisations using this simple and low-cost method.

The gold electrodes are created by spray deposition of gold nanoink (Fig. 2*c*). For this process, a borosilicate capillary micropipette with 1 μm diameter outer tip and 500 nm inner diameter is used to spray gold nanoink onto the substrate. Then the chip is heated to 350°C and annealed for 45 min to assure an ohmic contact (Fig. 2*d*). Alternatively, direct annealing by the focused laser is also possible. Electrical conduction inside the annealed nanoink pattern is of the order of $10^{-6}\,\Omega\,\mathrm{m}$ as was shown in previous works [16–18].

Induced-charge electro-osmosis [21, 22], where an electric field is applied down a capillary tube to generate a uniform plug flow driven by the slip at the surface, is used to spray the gold nanoink. To explain this effect, one can consider a liquid electrolyte, consisting of positive and negative particles in liquid solution. The interface between the electrolyte and the container wall generally forms a double layer in equilibrium, where a non-zero surface charge is screened by a very thin diffuse layer of excess ionic charge of width λ, the Debye screening length (typically 1–100 nm). The double layer is effectively a capacitor skin at the interface, which has a small voltage ζ across called the zeta potential. When a tangential electric field E_{ii} applied parallel to a flat surface, the electric field acts on ions in the diffuse part of the double layer, which drags the fluid to produce an effective slip velocity outside the double layer by the Helmholtz–Smoluchowski formula [23], $u_{11} = -\mu_E E_{11}$, where u_{11} is the tangential flow velocity through a flat surface channel, the constant of proportionality is $\mu_E = \varepsilon\zeta/\eta$ in terms of the permittivity ε and viscosity η of the fluid.

An electric field is created from the electrostatic charge between the capillary probe and the substrate. The created electric field triggers the colloidal spray and guides the direction of spray deposition. The spot diameter can be controlled by changing the distance between the probe tip and the substrate using piezoactuator robotic manipulators. The evaporation rate of bulk liquid ($C_{14}H_{30}$) at ambient conditions is slow and avoids clogging. However, the sprayed colloidal droplets evaporate rapidly from the increased surface-to-volume ratio. The spray method was also successfully experimented with another type of gold nanoink, containing 2–4 nm size nanoparticles in toluene solvents (C_7H_8) with a lower boiling point (110.6°C).

The main advantage of this method is that it does not require the conventional high electric potential between built-in electrodes. This non-contact spray method can deposit colloids onto any type of materials including dielectric or conducting materials but also on hydrophobic surfaces or rough ones. It can create patterned gold electrodes on the graphene and dielectric substrates without installing additional electrodes.

Fig. 3 shows the photo of gold nanoink spray process onto dielectric Pyrex substrate (Fig. 3*a*) and graphene (Fig. 3*b*). The pipette attached to the manipulator arm was controlled in the x–y plane to pattern an array of gold electrodes. The rate of spray deposition can be controlled by the distance between substrate and the pipette. In Fig. 3*a*, each electrode element is 2–6 μm in width and 15–20 μm in length. Fig. 3*b* demonstrates the patterning of multiple gold electrodes (diameter 2–6 μm) on the graphene.

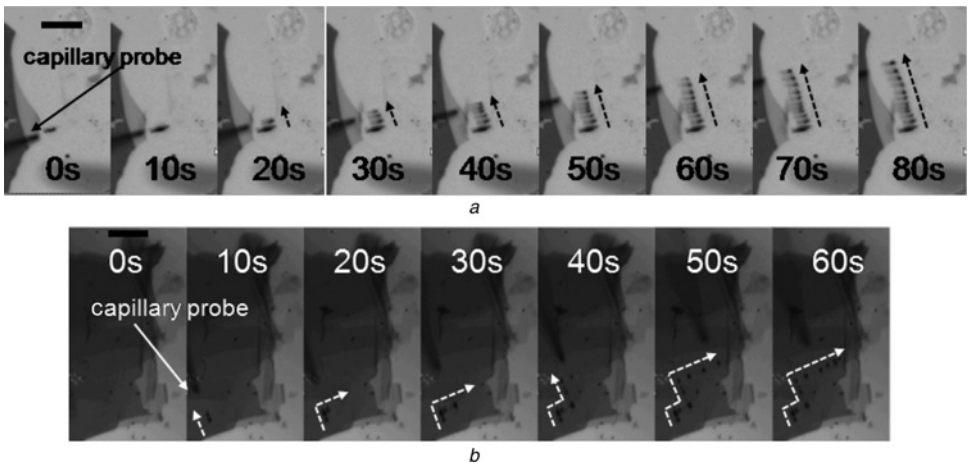

Figure 3 *Optical micrograph pictures of sprayed gold nanoparticle ink*

a Pictures of deposited gold nanoparticle ink onto glass substrate by spray method
b Spray-deposited gold nanoparticle ink onto graphene
Scale bar is 50 μm

Micro & Nano Letters, 2010, Vol. 5, Iss. 2, pp. 140–145
doi: 10.1049/mnl.2010.0012

Further size reduction can be achieved either by using pipette with smaller opening and/or by controlling the distance between the capillary probe and the substrate. Although the same substrate/pipette distance is used, in-plane deposited area (3–28 μm^2) on the graphene is much smaller than the one (30–120 μm^2) on the Pyrex. The round shape of the deposited area is attributed to the hydrophobicity of graphene enabling the self-assembly of tiny droplets. The arrows in Fig. 3 depicts the direction of the process. All steps were performed without refilling the gold nanoink. Focused IR laser heating was used for annealing process. The ink solidifies into gold electrodes and assures ohmic conductivity. An additional annealing by conventional oven heating confirmed that the laser based annealing gives the same ohmic conductivity.

Produced graphene chip's I–V characteristics are measured to verify proper electrical contact with a closed-loop power generator. Two different types of lasers were utilised to illuminate the graphene sample. The red laser was to point out the illuminated spot of the main IR laser. The electrical conductivity of graphene was increased with IR laser radiation (Fig. 4). First, absorption spectra of graphene were analysed. The absorbance of graphene was shown in the mid to near-IR spectral range from 0.2 eV (wavelength 6199 nm) to 1.2 eV (wavelength 1033 nm) [24] based on the conversion from photon energy to wavelength ($\lambda = hc/E$). For photon energy above 0.5 eV (wavelength between 1033 and 2479 nm), graphene yielded a spectrally flat optical absorbance of (2.3 ± 0.2)% and double in the case of a bilayer [24, 25]. This is consistent with previous studies [6, 26] and is compared with calculation and experimental data. The same universal absorbance spectra were also shown in graphite [27]. Recently, these optical absorbance spectra of few-layer graphene have a strong dependence on stacking sequence of graphene monolayers [28]. From these optical spectra of graphene, the wavelength (1480 nm) of the near-IR laser used for the experiment in this Letter is within the flat absorbance spectra (wavelength between 1033 and 2479 nm). Therefore it is confirmed that the demonstrated graphene photoelectric effect was triggered by the absorption of the near-IR laser (wavelength 1480 nm) used in this Letter.

Furthermore, the thermal heating of graphene caused by IR laser absorption was known to decrease the conductivity of graphene according to the literature [24, 29–31]. So, the thermal effect was excluded from the increased conductivity of graphene by IR laser. The measured I–V curve is shown in Fig. 4. The power when crossing 0 V source is calculated as 4.02 mV from the increased current (0.0121 mA) and intrinsic resistance (332.6 Ω). IR laser radiation heats the sample at around 60°C, but on the contrary to a known direct dependency between the graphene resistivity and the temperature, experiments show a clear inverse relation. In order to verify a hypothesis stating that the decrease in the resistivity is owing to a photoelectron effect, a second experiment is conducted. For this purpose, all external electric sources are disconnected from the chip, with the exception of the electrometer. A simple graphene source-drain circuit is configured by two micromanipulators with tungsten probe tips. In this configuration, IR laser is the only possible power source. The measured IR induced

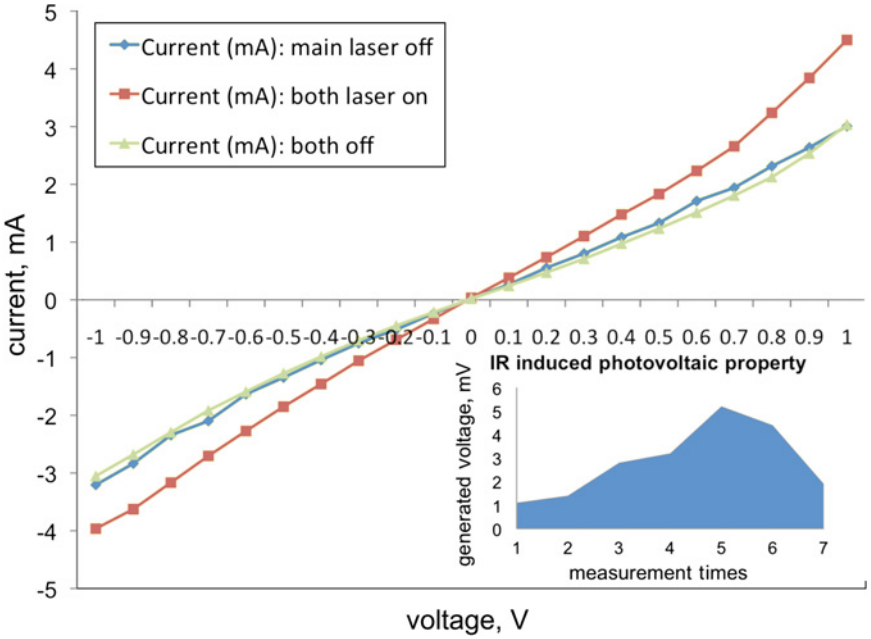

Figure 4 *I–V characteristic of IR-induced photoelectric effect*

The figure shows the I–V curve of an IR photodetector manufactured as described. IR laser was used as a main laser source and/or additional red laser was used to point out the IR laser-illuminated spot. Inset presents the generated photovoltaic voltage without additional power source

voltage, without any other power source, is found between 1.1 and 5.2 mV depending on the radiated area (see the inset of Fig. 4). The diameter of illuminated area by focused laser is estimated within the range of few microns approximately. These values are in good agreement with the shift in the resistance in the first configuration depicted in Fig. 4 and confirm the hypothesis on the photovoltaic properties of the graphene under IR radiation. This newly discovered property of graphene can be utilised as thin-film IR light sensors and optoelectronic transistors and can contribute to a new generation of solar cells.

2 Conclusion

The introduced gold nanoink spray process demonstrates the colloidal droplet deposition onto ultra-thin film hydrophobic 2D nanostructures such as graphene. The method does not require any additional pump, embedded electrodes or a high electrical potential. This process is also independent of the surface properties of the material and is controllable by the position control of the robotic manipulator or of the sample holder. The process is used to produce pure graphene devices and first experiments revealed the photocurrent effect generated by an IR laser radiation. These results reflect intrinsic optoelectronic properties of graphene as the production did not involve lithography or any other clean room process. The proposed process can be implemented to mass manufacture thin-film, transparent, flexible optoelectronic devices by robotic automation.

3 Acknowledgments

This work has been supported by ANR, the French National Agency of Research, through the NANOROL project. The authors thank Adrian Balan, Dr Rakesh Kumar and Prof. Abhay Shukla in IMPMC, UPMC, for valuable discussions and help with graphene sample preparation.

4 References

[1] NOVOSELOV K.S., GEIM A.K., MOROZOV S.V., *ET AL.*: 'Electric field effect in atomically thin carbon films', *Science*, 2004, **306**, pp. 666–669

[2] GEIM A.K., NOVOSELOV K.S.: 'The rise of graphene', *Nat. Mat.*, 2007, **6**, pp. 183–191

[3] AVOURIS P., CHEN Z., PEREBEINOS V.: *Nat. Nanotech.*, 2007, **2**, pp. 605–615

[4] ZHANG Y., TAN J.W., STORMER H.I., KIM P.: 'Experimental observation of the quantum Hall effect and Berry's phase in graphene', *Nature*, 2005, **438**, pp. 201–204

[5] WANG F., ZHANG Y., TIAN C., *ET AL.*: 'Gate-variable optical transitions in graphene', *Science*, 2008, **320**, pp. 206–209

[6] NAIR R.R., BLAKE P., GRIGORENKO A.N., *ET AL.*: 'Fine structure constant defines visual transparency of graphene', *Science*, 2008, **320**, p. 1308

[7] XIA F., MUELLER T., LIN Y., VALDES-GARCIA A., AVOURIS P.: 'Ultrafast graphene photodetector', *Nat. Nanotech.*, 2009, **4**, pp. 839–843

[8] LEVENDORF M.P., RUIZ-VARGAS C.S., GARG S., PARK J.: 'Transfer-free batch fabrication of single layer graphene transistors', *Nano Lett.*, 2009, **9**, pp. 4479–4483

[9] STANKOVICH S., DIKIN D.A., PINER R.D., *ET AL.*: 'Synthesis of graphene-based nanosheets via chemical reduction of exfoliated graphite oxide', *Carbon*, 2007, **45**, pp. 1558–1565

[10] LI X., WANG X., ZHANG L., LEE S., DAI H.: 'Chemically derived, ultrasmooth graphene nanoribbon semiconductors', *Science*, 2008, **319**, pp. 1229–1232

[11] SI Y., SAMULSKI E.T.: 'Synthesis of water soluble graphene', *Nano Lett.*, 2008, **8**, pp. 1679–1682

[12] LI X., ZHANG G., BAI X., *ET AL.*: 'Highly conducting graphene sheets and Langmuir-Blodgett films', *Nat. Nanotechnol.*, 2008, **3**, pp. 538–542

[13] HERNANDEZ Y., NICOLOSI V., LOTYA M., *ET AL.*: 'High-yield production of graphene by liquid-phase exfoliation of graphite', *Nat. Nanotechnol.*, 2008, **3**, pp. 563–568

[14] BURG B.R., LUTOLF F., SCHNEIDER J., SCHIRMER N.C., SCHWAMB T., POULIKAKOS D.: 'High-yield dielectrophoretic assembly of two-dimensional graphene nanostructures', *Appl. Phys. Lett.*, 2009, **94**, article no. 053110, 3pp.

[15] HWANG G., HASHIMOTO H., BELL D.J., DONG L., NELSON B.J., SCHON S.: 'Piezoresistive InGaAs/GaAs nanosprings with metal connectors', *Nano Lett.*, 2009, **9**, (2), pp. 554–561

[16] CHOI T.Y., POULIKAKOS D., GRIGOROPOULOS C.P.: 'Fountain-pen-based laser microstructuring with gold nanoparticle inks', *Appl. Phys. Lett.*, 2004, **85**, (1), article no. 13

[17] DOCKENDORF C., POULIKAKOS D., HWANG G., NELSON B.J., GRIGOROPOULOS C.P.: 'Maskless writing of a flexible nanoscale transistor with Au-contacted carbon nanotube electrodes', *Appl. Phys. Lett.*, 2007, **91**, article no. 243118, 3pp.

[18] DOCKENDORF C., CHOI T.Y., STEINLIN M., POULIKAKOS D.: 'Individual carbon nanotube soldering with gold nanoink deposition', *Appl. Phys. Lett.*, 2007, **90**, article no. 193116, 3pp.

[19] SCHIRMER N.C., SCHWAMB T., BURG B.R., HOTZ N., POULIKAKOS D.: 'Controlled free-form fabrication of nanowires by dielectrophoretic dispension of colloids', *Appl. Phys. Lett.*, 2009, **95**, (3), article no. 033111, 3pp.

doi: 10.1049/mnl.2010.0012

[20] SHUKLA A., KUMAR R., MAZHER J., BALAN A.: 'Graphene made easy: high quality, large-area samples', *Solid State Commun.*, 2009, **149**, pp. 718–721

[21] BAZANT M.Z., SQUIRES T.M.: 'Induced-charge electrokinetic phenomena: theory and microfluidic applications', *Phys. Rev. Lett.*, 2004, **92**, article no. 066101

[22] LEVITAN J.A., DEVASENATHIPATHY S., STUDER V., *ET AL.*: 'Experimental observation of induced-charge electro-osmosis around a metal wire in a microchannel', *Coll. Surf. A*, 2005, **267**, pp. 122–132

[23] HUNTER R.J.: 'Zeta potential in colloid science principles and applications' (Academic Press, 1981)

[24] MAK K.F., SFEIR M.Y., WU Y., LUI C.H., MISEWICH J.A., HEINZ T.F.: 'Measurement of the optical conductivity of graphene', *Phys. Rev. Lett.*, 2008, **101**, article no. 196405, 4pp.

[25] YANG L., DESLIPPE J., PARK C., COHEN M.L., LOUIE S.G.: 'Nonmagnetic impurity resonances as a signature of sign-reversal pairing in FeAs-based superconductors', *Phys. Rev. Lett.*, 2009, **103**, article no. 186402

[26] KATSNELSON M.I.: 'Optical properties of graphene: the fermi-liquid approach', *Europhys Lett.*, 2008, **84**, article no. 37001

[27] KUZMENKO A.B., HEUMEN E., CARBONE F., MAREL D.: 'Universal optical conductance of graphite', *Phys. Rev. Lett.*, 2008, **100**, article no. 117401

[28] MAK K.F., SHAN J., HEINZ T.F.: 'Electronic structure of few-layer graphene: experimental demonstration of strong dependence on stacking sequence', http://arxiv.org/ftp/arxiv/papers/1002/1002.2225.pdf/ (accessed 2010)

[29] BOLOTIN K.I., SIKES K.J., HONE J., STORMER H.L., KIM P.: 'Temperature dependent transport in suspended graphene', *Phys. Rev. Lett.*, 2008, **101**, article no. 096802

[30] XU W., PEETERS F.M., LU T.C.: 'Dependence of resistivity on electron density and temperature in graphene', *Phys. Rev. B*, 2009, **79**, article no. 073403, 4pp.

[31] AKTURK A., GOLDSMAN N.: 'Unusually strong temperature dependence of graphene electron mobility'. Proc. Int. Conf. on Simulation of Semiconductor Processes and Devices, Hakone, Kanagawa, Japan, 2008, pp. 173–176